

Kinetics of Graphite Oxidation: Monolayer and Multilayer Etch Pits in HOPG Studied by STM

Forrest Stevens, Lisa A. Kolodny, and Thomas P. Beebe, Jr.*

The University of Utah, Department of Chemistry, Salt Lake City, Utah 84112

Received: April 28, 1998; In Final Form: October 13, 1998

Oxidation experiments using a particular grade of highly oriented pyrolytic graphite have allowed observation of large numbers of both monolayer and multilayer etch pits on the same samples, formed under identical conditions. Scanning tunneling microscopy was used to measure pits produced after various etch times, temperatures, and O₂ pressures. From these data pit growth rates, activation energies, and reaction orders were derived. Although multilayer pits were observed to grow over 3 times faster than monolayer pits in air, both types of pits had the same activation energy. Multilayer etch pits were sometimes observed to form at screw dislocations in the graphite but were also seen in the absence of such defects. The experimentally determined reaction rates and activation energies were not consistent with a direct reaction of edge-carbon atoms with atmospheric oxygen, but instead suggest a chain reaction or preequilibrium process. A mechanism for oxidation of multilayer pits involving reaction of partially oxidized sites on adjacent graphite layers is suggested.

Introduction

Understanding the oxidation of carbon is of great fundamental and applied interest for improving processes such as production of liquid or gaseous fuels from coal, removing carbon deposits from catalysts, and diamond thin-film growth. Studies of carbon oxidation are often performed on graphite to take advantage of its known and regular structure, that is easier to model than chars or other samples of poorly defined structure. The oxidation of graphite has proved complex and is only partly understood. Oxidation of highly oriented pyrolytic graphite (HOPG) produces etch pits on the basal plane, that can be one or many graphite layers deep. Early optical studies showed only macroscopically wide and deep etch pits.^{1,2} Later, edge decoration and electron microscopy revealed monolayer etch pits,^{3,4} that have also been observed by STM.^{5,6} Multilayer etch pits have also been studied by STM, but they are normally observed so infrequently that only limited data could be obtained on them. There have been a few reports of the relative growth rates for monolayer and multilayer etch pits or steps, often using indirect measures of multilayer growth rates. Measured growth rates have ranged from equal⁷ to 100 times greater for multilayer pits.³ It has also been observed that monolayer and multilayer pits made by heating in air display different shapes, with monolayer pits generally being circular, while many multilayer pits are hexagonal. Comparison of reported results is often difficult due to varying etching conditions and types of graphite used.

Our interest in the oxidation of graphite is due to its frequent use as an STM substrate,⁸ and to a desire to find empirical methods for producing various types of etch pits for use as "molecule corrals."^{9,10} By using a lower grade of HOPG containing more defects, we were able to image a large number of multilayer etch pits, determine their growth rates, and show that while some multilayer pits form at screw defects in the

HOPG, others do not. By studying monolayer and multilayer etch pits on the same sample, we could directly compare their relative growth rates and shapes. Activation energies and reaction orders for monolayer and multilayer etch pits were also determined.

Experimental Section

The STM used in these studies is custom built and has been described elsewhere.¹¹ Typical scanning conditions used were: 0.60 V (tip positive), 160 pA. Images were acquired in both constant-height and constant-current (topographic) mode, using mechanically cut tips of Pt/Ir (80:20). All images were acquired at room temperature, after allowing the samples to cool.

Highly oriented pyrolytic graphite, grades ZYA, ZYB, and ZYC, was supplied by Dr. Arthur W. Moore of Union Carbide. ZYA and ZYB grades have similar crystallite sizes and were not distinguished, while ZYC grade has a smaller crystallite size and more defects than the other grades.¹² HOPG was etched in air using a Lindberg Hevi-Duty tube furnace. The HOPG sample was placed in the center of a 2.5 cm × 60 cm horizontal quartz tube; both ends of the tube were left open, and no effort was made to either cause or prevent air flow (except for pressure-dependence studies; see below). Most experiments were conducted at 650 °C as measured by a thermocouple inside the furnace. For activation energy calculations, additional experiments were conducted between 500 and 800 °C.

An additional set of experiments was performed by admitting a measured mixture of oxygen and nitrogen in one end of the tube (that was sealed except for the gas inlets) and allowing the gases to flow through the reaction tube and out the other end (that was left open). The total gas flow was kept constant at 3.0 mL/s. By measuring the reaction rate at different temperatures and with different gas ratios, reaction rate orders could be measured with respect to O₂ partial pressure. Nitrogen: oxygen ratios ranged from 64:36 to 93.3:6.7. A "blank" reaction using pure nitrogen showed no measurable oxidation of the sample.

* Phone: (801) 581-5383. Fax: (801) 581-8433. E-mail: beebe@chemistry.chem.utah.edu.

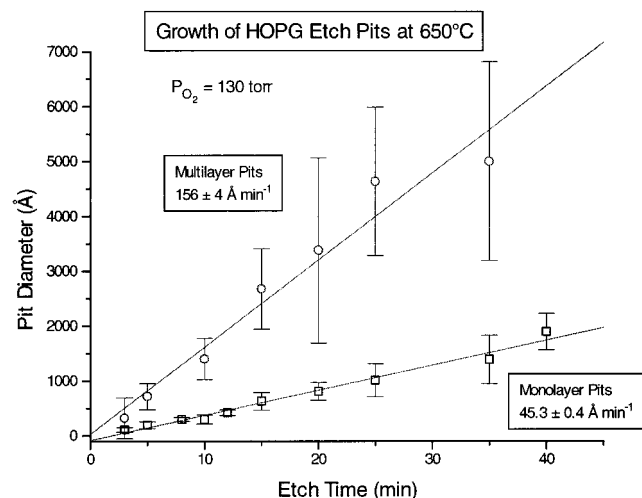


Figure 1. Plot of pit diameter vs etch time for monolayer and multilayer etch pits at 650 °C. 1σ error bars are shown for each etch time. A total of 3713 monolayer pits and 528 multilayer pits were measured by STM.

Results

Monolayer Etch Pits. Most monolayer etch pits were observed on ZYB grade HOPG at 650 °C in air. Monolayer pits on ZYC grade HOPG appeared indistinguishable from monolayer pits on ZYB grade HOPG formed under similar conditions, but the higher defect density on ZYC grade HOPG made the monolayer pits more difficult to observe than on the ZYB grade HOPG.

Previous reports have found that the size of monolayer etch pits could be controlled by varying the etch time, with pit diameter increasing linearly at a rate of $52 \text{ Å} \cdot \text{min}^{-1}$ (650 °C)⁵ or $19\text{--}30 \text{ Å} \cdot \text{min}^{-1}$ (650 °C).¹³ We observed a similar rate of $45.3 \pm 0.3 \text{ Å} \cdot \text{min}^{-1}$ at 650 °C in air ($N = 3713, \pm 1\sigma$), as shown in Figure 1. A linear fit to a plot of the diameter (y-axis) vs time (x-axis) data does not intersect the origin but shows an x-axis intercept of $1.2 \pm 0.1 \text{ min}$, similar to the previously reported value of 1.7 min at the same temperature.¹³ This nonzero intercept presumably reflects some initiation time before etching begins. While the size of the etch pits produced after a given oxidation time was consistent over many hundreds of trials and samples, the pit density was less readily controlled. The reported technique of using “thermal shocks” (placing the sample in the oven for 1 min, removing, and repeating as desired) did increase the density of etch pits, but the amount of increase was highly variable and not reproducible. By studying samples that had been exposed to varying numbers of thermal shocks, followed by etching, we were able to determine that no significant pit growth occurs during thermal shocks. A plot of average pit size vs number of thermal shocks shows no tendency for pit size to increase with the number of thermal shocks, as would be expected if any growth occurred during each thermal shock. This confirms that an induction period (of at least 1 min) precedes growth of the monolayer pits.

A previous report¹⁴ indicated that monolayer pit growth rates were related to pit density, with larger pits being formed at lower pit densities. This effect was reported to level off at pit densities above $\sim 10 \mu\text{m}^{-2}$. We noted a weak tendency for the largest pits to be found on samples having densities below $\sim 4 \mu\text{m}^{-2}$, but the effect was of nearly the same order as the scatter in the data. Most of our samples had pit densities well above $10 \mu\text{m}^{-2}$.

Multilayer Etch Pits. Heating HOPG in air has long been known to create micron-scale hexagonal etch pits, which can

TABLE 1: HOPG Multilayer Pit Densities (650 °C in Air)

type of HOPG	area Scanned (μm^2)	no. of multilayer pits obsd	multilayer pits per μm^2
ZYC etched	1007	518	0.51
ZYC not etched	311	1 ^a	0.00
ZYB etched	245	3	0.01
ZYB not etched	207	0	0.00

^a One small, round, deep pit was observed. Its origin is unclear.

be observed optically.^{1,2,15} Similar etch pits (deeper than a monolayer, and often hexagonal) have been observed by STM, but usually occur at such low densities that it has been difficult to collect a statistically meaningful amount of data on them.^{6,13,16,17} Multilayer pits have also been created by etching HOPG after bombardment with polyatomic ions,^{18–20} but these pits have not yet been systematically studied. While etching ZYB grade HOPG to produce monolayer pits, we observed a few multilayer pits, but only rarely. However, we also had access to samples of ZYC grade HOPG, which contain a much higher density of defects, and etching this material was found to produce a ~ 50 times higher density of large multilayer etch pits, as shown in Table 1. Although the multilayer pits produced on the different grades of HOPG appeared to be similar, too few multilayer pits were observed on the ZYB grade graphite to make a statistically meaningful comparison to those seen on the ZYC grade graphite.

Prior reports have disagreed as to the relative etch rates of multilayer edges as compared to monolayer edges. Evans³ reported that multilayer edges grew 100 times faster than monolayer edges at 0.01 Torr of O_2 and 840 °C. Others have also reported that multilayer edges or pits grow faster than monolayer edges or pits by factors of 4.3,^{6,16} 20 (5 Torr),¹⁶ 8 (700 °C, 150 Torr),²¹ and “much larger and deeper than the monolayer etch pits.”¹³ However, Tracz⁷ reported the rates of monolayer and multilayer recession to be nearly the same at 670 °C and 150 Torr of O_2 . The various temperatures, pressures, samples, and methods of measuring multilayer growth rates used in the literature make it difficult to compare these values directly. As seen in Figure 1, we have found multilayer pits to grow 3.4 times faster than monolayer pits, at a rate of $156 \pm 4 \text{ Å} \cdot \text{min}^{-1}$ at 650 °C in air (130 Torr O_2) as compared to $45.3 \pm 0.4 \text{ Å} \cdot \text{min}^{-1}$ for monolayer pits under the same conditions.

The origin of these multilayer etch pits is unclear, although they presumably occur at line defects that cut through many graphite layers. Some multilayer pits observed by optical methods,²² or by electron microscopy,²³ have been shown to occur at screw defects, and multilayer pits observed by STM have been presumed to also occur at screw defects. We have found that in fact some but not all multilayer etch pits occur at screw defects. Pits located on screw defects can be recognized by a single step radiating away from the pit,^{22,23} as in Figure 2. In contrast, the large pit in Figure 3 does not show any radiating steps, and so did not form at a screw defect. Pits that intersected multiple steps could not be classified as occurring on or not-on a screw defect. A total of 132 pits on screw defects were observed, representing 25% of all multilayer pits observed, or 68% of the pits that could be classified as on or not-on screw defects. It is not clear what features besides screw defects allow the formation of multilayer etch pits, although impurities are one possibility. Etch rates for screw and nonscrew pits were calculated separately and were found to be nearly the same, with pits not on screw defects etching at $173 \pm 16 \text{ Å} \cdot \text{min}^{-1}$, and pits on screw defects etching at $150 \pm 6 \text{ Å} \cdot \text{min}^{-1}$ (both at 650 °C in air).

The growth rate for multilayer pits was determined by measuring the increase in pit diameter, even though the total

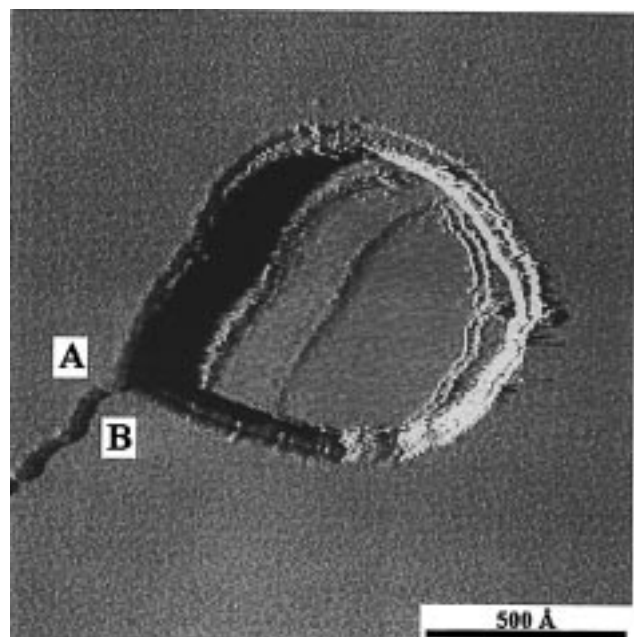


Figure 2. STM image of a multilayer pit etched for 5 min at 650 °C. The single step radiating from this pit identifies it as having formed at a screw defect. Points A and B are separated by a step in the surface, but by traveling clockwise around the pit, it is possible to move from A to B without crossing any steps. Image is 1570 Å on a side, taken at 0.59 V, 162 pA, constant height mode. Reduced to 70% for publication.

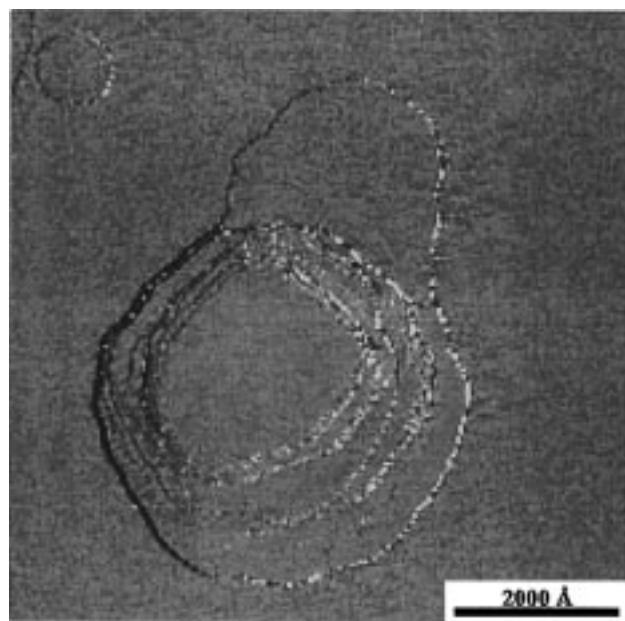


Figure 3. STM image of a multilayer pit (center) and a monolayer pit (upper left) etched for 25 min at 650 °C. In this case, the multilayer pit did not form at a screw defect, since no steps intersect the edge of the pit. Image is 7500 Å on a side, taken at 0.58 V, 166 pA, constant height mode. Reduced to 70% for publication.

number of carbon atoms removed per unit time will be much larger for deeper pits. Using the diameter as a measure of growth rate was based on the assumption that the etch rate would be proportional to N_{edge} , the number of edge carbon atoms, that is

$$\text{rate} = kN_{\text{edge}} \quad (1)$$

Since the number of edge carbon atoms is directly proportional to pit depth, the rate of growth of pit diameter was

TABLE 2: Kinetic Data for HOPG Etching in Air^a

type of etch pit	E_a (kJ·mol ⁻¹)	A (s ⁻¹) × 10 ⁻¹¹
monolayer	168 ± 5	1.6 ± 1
multilayer (all)	175 ± 3	12 ± 5
multilayer (on screw defect)	165 ± 9	3.2 ± 4
multilayer (not on screw defect)	180 ± 9	29 ± 35

^a Rate = $Ae^{-(E_a/RT)}$. Errors are from standard errors from least-squares fit to the data.

expected to be independent of pit depth in the absence of some limiting reactant. The fact that pit diameter plotted against etch time produces a linear plot supports this hypothesis, but we also wished to study the effects of pit depth more directly.

The true absolute depths of multilayer etch pits were difficult to measure for several reasons. First, the STM height scale is difficult to calibrate at the 10–100 Å range due to lack of appropriate standards.²⁴ Second, a single etch pit frequently showed variations in depth, for example due to one or more steps intersecting the etch pit. Finally, the finite size of the STM tip could cause some cases in which the true bottom of the etch pit may not have been measured. Nevertheless, we felt that any *trends* in pit depth should still be observable, given a reasonably large sample size. Linear regression of pit depth vs pit diameter was done for 26 sets of pits, where each set was observed on the same sample with the same tip and contained 8–42 measurements of pits (total 431). Correlation (R) values for these sets ranged from -0.67 to +0.84, but 70% were within the range of ±0.50, and the average was only 0.14, indicating little consistent correlation between pit depth and diameter. Linear regression of depth vs diameter plots showed both positive and negative slopes, with an average slope of 0.0. While the difficulties in measuring depths accurately mean that we cannot rule out a correlation between pit depth and diameter, we saw no evidence for such a correlation. A previous report of shallow etch pits found an increase in growth rate with depth up to four monolayers, but no change in growth rate for pits deeper than four monolayers.^{18,19}

There was a weak tendency for pit depth to increase with time. Linear regression of pit depth vs time for all multilayer pits produced a slope of $4.8 \pm 0.4 \text{ Å} \cdot \text{min}^{-1}$ with an R value of 0.50. While this suggests a gradual deepening of etch pits, both deep and shallow multilayer pits were observed at each etch time. Thus it is possible that the distribution of pit depths reflects the distribution of depths for the trans-layer defects that apparently give rise to multilayer etch pits. The slight tendency for deeper pits to be observed after longer etch times may be due to incomplete etching of some defects at short etch times. This would bias pits produced by short etch times toward shallower depths, as the deeper defects would not be completely etched.

Activation Energies. Although most of the work in this study was done at an oven temperature of 650 °C, additional etching was done at 500, 575, 725, and 800 °C in order to determine activation energies for pit growth, as shown in Table 2. Only ZYC grade HOPG was used at these temperatures. By measuring pit growth rates for monolayer and multilayer pits at each temperature, and plotting $\ln(\text{rate})$ vs T^{-1} , as shown in Figure 4, it was determined that the activation energy for monolayer pits²⁵ is $168 \pm 5 \text{ kJ} \cdot \text{mol}^{-1}$, and for multilayer pits, $175 \pm 3 \text{ kJ} \cdot \text{mol}^{-1}$. These values are essentially the same within experimental error. Preexponential factors were found to be significantly different for monolayer and multilayer pits (Table 2). These results show that although monolayer and multilayer etch pits have similar or identical barriers to reaction, atoms at multilayer pit edges experience more reaction opportunities per unit time. Kinetic

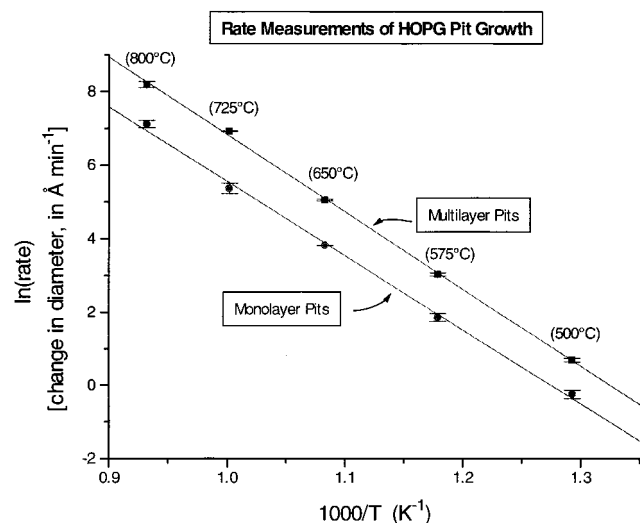


Figure 4. Arrhenius plot for monolayer and multilayer etch pits. The rate ($\text{rate} = Ae^{-(E_a/RT)}$) of change of pit diameter (in $\text{\AA}\cdot\text{min}^{-1}$) was used as a measurement of the etch rate. At least three different etch times were used to determine the rate at each temperature. For monolayer pits, $E_a = 168 \pm 5 \text{ kJ}\cdot\text{mol}^{-1}$ and $A = (1.6 \pm 1) \times 10^{11} \text{ s}^{-1}$. For multilayer pits, $E_a = 175 \pm 3 \text{ kJ}\cdot\text{mol}^{-1}$ and $A = (12 \pm 5) \times 10^{11} \text{ s}^{-1}$. Error bars are the standard errors on the least-squares fit to the data at each temperature.

parameters were also determined for multilayer pits on, and not on, screw defects. Unfortunately, most pits could not be identified unambiguously as being on, or not on, screw defects. Consequently, data quality was poor and no definite conclusions could be reached (Table 2).

In air, the ratio of multilayer to monolayer etch rates increased from 2.6 at 500 °C to 4.7 at 725 °C, but then decreased to 2.9 at 800 °C, so it is not clear if any real trend exists. The average rate ratio was 3.4 ± 0.8 over this temperature range.

Discussion

The observed etch rate for pits on graphite can be used to determine the reaction rate, commonly expressed as number of carbon atoms reacted per available (edge) carbon atom per unit time. At 650 °C values of $0.5\text{--}0.9 \text{ s}^{-1}$,²⁶ 0.5 s^{-1} ,¹³ and 0.93 s^{-1} ¹⁴ have been reported (all for monolayer pits).²⁷ We calculated rates of $0.288 \pm 0.002 \text{ s}^{-1}$ for monolayer pits and $0.99 \pm 0.02 \text{ s}^{-1}$ for multilayer pits at 650 °C in air.

The simplest mechanism for HOPG oxidation would be direct reaction with oxygen (an O_2 molecule collides with an edge carbon, forming CO or CO_2). In this case, a maximum reaction rate can be calculated from the number of oxygen molecules striking each carbon atom per second, and the fraction of oxygen molecules having at least the activation energy of the reaction. The activation energy of graphite oxidation has been studied by many groups over the years, but the values reported have varied from below 100 to over 300 $\text{kJ}\cdot\text{mol}^{-1}$. However, more recent studies (since 1980) have spanned a narrower range, from 127⁶ to 222 $\text{kJ}\cdot\text{mol}^{-1}$.²⁸ Three recent studies^{6,16,29} have all obtained values for the activation energy of about 130 $\text{kJ}\cdot\text{mol}^{-1}$. The present results of 168 ± 5 (monolayer) and $175 \pm 3 \text{ kJ}\cdot\text{mol}^{-1}$ (multilayer) are somewhat higher than this value but are near the center of the range of other recently reported values. Gerasimov³⁰ has calculated the E_a of graphite oxidation to be 172 $\text{kJ}\cdot\text{mol}^{-1}$.

For an O_2 partial pressure of 0.16 atm at 650 °C, the rate of collisions of O_2 molecules with a surface is $2.57 \times 10^{22} \text{ cm}^{-2} \text{ s}^{-1}$. Or, since each carbon atom in the graphite basal plane

occupies 2.62 \AA^2 , the collision rate with graphite is 6.73×10^6 per carbon atom per second. The fraction of colliding molecules having kinetic energy equal to or greater than the activation energy can be found by starting with the velocity-based Maxwell–Boltzmann equation:

$$f(v) = 4\pi \left(\frac{M_w}{2000\pi RT} \right)^{3/2} v^2 e^{-M_w v^2 / 2000RT} \quad (2)$$

where R = gas constant, M_w = molar mass of an oxygen molecule, v = molecular velocity, and T = temperature.

And by making the substitutions

$$C = 4\pi \left(\frac{M_w}{2000\pi RT} \right)^{3/2}, \quad x = v, \quad a = \left(\frac{M_w}{2000RT} \right)^{1/2} \quad (3)$$

the equation can then be rewritten as

$$f(x) = Cx^2 e^{-a^2 x^2} \quad (4)$$

which can be integrated according to standard tables:³¹

$$\int f(x) dx = C \left\{ -\frac{1}{2a^2} x e^{-a^2 x^2} + \frac{\sqrt{\pi}}{4a^3} \text{erf}(ax) \right\} \quad (5)$$

Using this integrated Maxwell–Boltzmann equation (evaluated by computer), at 650 °C the fraction of O_2 molecules having a kinetic energy of at least 172 $\text{kJ}\cdot\text{mol}^{-1}$ (the average of the two experimental values) is 1.01×10^{-9} .³² Thus, if every O_2 molecule having at least the measured activation energy reacted with one carbon atom when it struck the surface, a reaction rate of 0.007 reactions per edge carbon atom per second would be expected (the product of the collisions per carbon atom per second and the fraction of O_2 molecules that have kinetic energy of at least 172 $\text{kJ}\cdot\text{mol}^{-1}$: 6.73×10^6 and 1.01×10^{-9}). At 650 °C the experimental values determined here are larger than this rate by a factor of 42 for monolayer pits, and by a factor of 146 for multilayer pits. The ratio of predicted to experimental rates was nearly constant over the range of temperatures studied, averaging 46 ± 9 for monolayer pits and 153 ± 27 for multilayer pits. This would appear to rule out a direct-collision oxidation mechanism and supports alternatives such as chain-reaction³³ or preequilibrium^{34,35} mechanisms.

Monte Carlo computer modeling of monolayer pits³⁶ by varying the reaction probabilities of different types of edge carbon atoms has shown that circular monolayer pits can be well reproduced over a range of parameters, but hexagonal multilayer pits could only be poorly reproduced. This suggests that the difference between circular monolayer and hexagonal multilayer pits is not simply due to some change in the oxidation rates of different types of edge atoms but is due to an interaction between the stacked HOPG edges.

Our finding that the growth rate of multilayer pits has little or no dependence on the pit depth shows that whatever edge–edge interaction is present, the effect is not cumulative. That is, for both monolayer and multilayer pits, the etch rate is proportional to the number of edge carbon atoms, but the proportionality constant differs between monolayer and multilayer pits.

$$\text{rate} = kN_{\text{edge}}, \quad k_{\text{mono}} \neq k_{\text{multi}} \quad (6)$$

While this change is likely due to some edge–edge effects between the adjacent HOPG edges of the multilayer pits, these effects are not additive. There is a clear difference in reaction

TABLE 3: Monolayer and Multilayer Etching Reaction Order, m , Rate = $k(\% \text{ O}_2)^m$, from Slope of $\ln(\% \text{ O}_2)$ vs $\ln(\text{rate})$

type of pit	reaction order	
	650 °C	725 °C
monolayer	0.99 ± 0.14	0.87 ± 0.13
multilayer	0.22 ± 0.05	0.86 ± 0.14

rate between monolayer and multilayer pits, but no significant differences were noted between shallow and deep multilayer pits.

Reaction Order. Yang³⁷ has reported that the growth rate for monolayer pits was half-order in O_2 pressure from 650 to 850 °C, while the bulk etch rate (that was mostly due to multilayer etching) changed from half-order in O_2 at 650 °C to first-order in O_2 at 850 °C. However, other researchers have measured the order of O_2 pressure dependence to be 0.2–0.3 (multilayer pits),² 0.5–0.6 (bulk graphite),^{35,38} or 1 (monolayer pits,¹⁶ thin film of char,³⁴ and bulk graphite³⁹). As with activation energies, the differing samples and reaction conditions make it difficult to compare these literature values directly.

However, there is some additional support for a difference in O_2 reaction order between monolayer and multilayer etch pits. Chu¹⁶ has noted that in O_2 , multilayer pits were 4.3 times larger than monolayer pits at “high” pressures, but 20 times larger at 5 Torr. An increasing difference in etch rates at low pressure is also consistent with Evans’ result that multilayer pits grew 100 times faster than monolayer pits.³ This is a much larger difference than anyone else has reported, but Evans was also working at much lower pressures (0.01 Torr O_2) than others.

The results of our pressure-dependence experiments are in basic agreement with previous results. At 725 °C, both monolayer and multilayer pits showed reaction orders near unity, as shown in Table 3. However, at the lower temperature of 650 °C, monolayer pits still showed a reaction order of 1, while multilayer pits showed a much reduced reaction order. This had a great effect on the ratios of monolayer to multilayer etch rates.

The change in reaction order for multilayer pits shows that the multilayer reaction mechanism changes between the two temperatures. At lower temperatures, the multilayer oxidation mechanism appears to be less sensitive to pressure than the monolayer reaction mechanism is, causing increasing disparities between monolayer and multilayer pit size as the O_2 pressure decreases.

A clue to the mechanism at lower temperature has been provided by Walker et al.⁴⁰ who used isotopically labeled oxygen to show that the primary mechanism for forming CO_2 from Graphon (graphitized carbon black) involves reactions between surface-bound (chemisorbed) oxygen atoms. Although the details of this reaction are not known, it is reasonable to assume that CO_2 can only form from pairs of adjacent (or nearby) chemisorbed O atoms. If a similar mechanism operates in the oxidation of graphite, then the differences between monolayer and multilayer etching are consistent with reactions involving chemisorbed O atoms on adjacent graphite sheets. If O atoms on adjacent sheets can indeed react, this would explain why multilayer pits etch at a faster rate than monolayer pits, and why monolayer and multilayer etching exhibit different O_2 pressure dependences.

On a monolayer edge, an O atom could only react with O atoms chemisorbed on either side along the monolayer edge. On a multilayer edge, an O atom could react with O atoms on either side along the same edge, or with O atoms on adjacent edges, and this would increase the possibilities for reaction. This

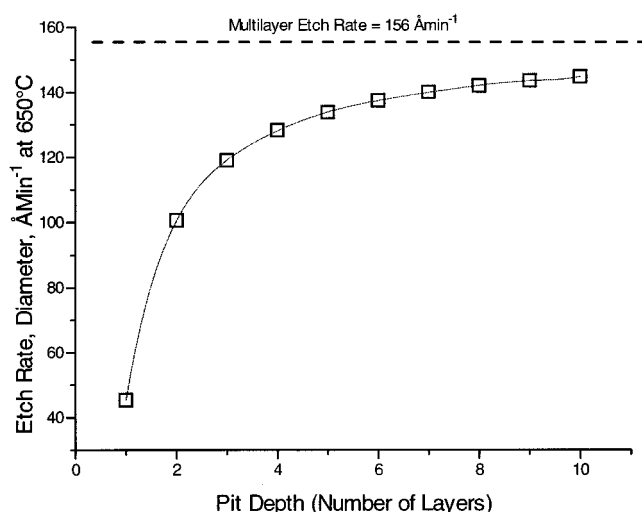


Figure 5. Plot of predicted etch rate as a function of multilayer pit depth, based on rate acceleration by adjacent layers, as discussed in the text. Note that etch rate is predicted to increase with pit depth only for very shallow pits; for pits deeper than about four layers, etch rate is predicted to be nearly independent of pit depth, as observed.

mechanism would also explain the lack of a depth dependence on etch rate, since an O atom could only react with atoms on the two adjacent sheet edges, and the presence or absence of additional edges beyond the nearest would have no effect on the reaction rate.

In addition, this mechanism would explain the differing pressure dependences of monolayer and multilayer etch pits. As the O_2 pressures drops, the number of chemisorbed oxygen atoms present at any time would also decrease, and the oxidation rate would decrease because fewer O atoms would be adjacent to each other. However, because multilayer edges have more possibilities for adjacent sites, the reaction rate for multilayer edges would drop more slowly as the chemisorbed O atoms become scarcer. It is not clear whether O atoms chemisorbed to HOPG step edges are fixed or mobile, but the above argument is qualitatively the same in either case.

If the increase in etch rate seen in multilayer etch pits is indeed due to reaction between sites on adjacent edges, then we can predict the dependence of etch rate on pit depth. We define x to be the etch rate of a monolayer edge and y to be the increase in etch rate caused by one adjacent edge. Furthermore, we assume that the effect is cumulative; that is, an edge between two edges will have a rate of $x + 2y$. Then the average etch rate of a pit n graphite layer deep will be

$$\text{rate} = x + (2 - 2/n) \cdot y \quad (7)$$

Clearly, for $n \gg 2$, the etch rate will converge to $x + 2y$, and appear to be independent of n . From our measured monolayer and multilayer etch rates we can determine that at 650 °C, $x = 45.3 \text{ Å} \cdot \text{min}^{-1}$ and $y = 55.3 \text{ Å} \cdot \text{min}^{-1}$, when rate is expressed as a change in diameter per unit time. A plot of the predicted etch rate vs pit depth is shown in Figure 5. Although the etch pits we measured were too deep to test this prediction, Bräuchle^{18,19} has reported that at a temperature of 900 K (627 °C), pit etch rates increase with depth up to a depth of four monolayers, a fact that is in qualitative agreement with the prediction shown in Figure 5, since $n = 4$ is approximately where the etch rate levels off and becomes independent of pit depth.

The oxidation of graphite is undoubtedly complex, and some reaction pathways produce CO as well as the CO_2 considered above. However, a reaction between neighboring chemisorbed

oxygen atoms, on the same or on adjacent HOPG sheets, explains many of the differences observed between monolayer and multilayer etch pits measured on the same graphite samples.

Conclusions

By using a grade of HOPG that contains more defects, a large number of multilayer etch pits were observed and their properties could be compared to monolayer etch pits. The speculation that multilayer etch pits form on screw defects has been shown to be true in some cases, but multilayer etch pits can also form in the absence of screw defects. The multilayer pits on these samples grew at a rate 3.4 times faster than the monolayer etch pits at 650 °C in air, and the growth rate was independent of pit depth.

Measuring etch rates at different temperatures allowed the calculation of activation energies that were found to be the same, within experimental error, for both monolayer and multilayer etch pits. Pressure-dependence studies clearly showed that the reaction mechanism for multilayer pits changes from low-order in oxygen at lower temperature to near first order at higher temperatures, while the reaction order for monolayer pits remained near first-order at both temperatures observed.

Using the measured activation energy, a maximum direct-collision reaction rate was calculated and was found to be much smaller than the experimentally observed reaction rate. This demonstrates that the mechanism of HOPG oxidation is not a direct combination of oxygen and edge carbons but may rather involve a chain reaction or preequilibrium. Many of the observed differences between monolayer and multilayer etch pits can be explained on the basis of reactions between neighboring chemisorbed O atoms, if reaction is allowed between atoms on adjacent HOPG sheets.

While multilayer etch pits are infrequent, especially on higher grades of graphite, their depth and faster growth rate means that a relatively large number of carbon atoms are oxidized at these sites. Thus, an understanding of multilayer etch pits is important to understanding graphite oxidation. In addition, it is possible that these multilayer pits might be made to serve some function as nanoscale or microscale "containers" in a similar manner as the monolayer etch pits have been used,^{9,41} but with an added depth dimension. ZYC grade HOPG holds great promise in improving understanding of the HOPG oxidation process, as it readily allows observation of both monolayer and multilayer etch pits on the same sample.

Acknowledgment. This work was supported by the National Science Foundation (CHE-9357188), the Camille and Henry Dreyfus Foundation, and the Alfred P. Sloan Foundation. L.A.K. was a visitor from Notre Dame University and was supported by the 1998 NSF REU grant no. CHE 9531410.

References and Notes

- (1) Hughes, E. E. G.; Thomas, J. M. *Nature* **1962**, *193*, 838–840.
- (2) Thomas, J. M.; Hughes, E. E. G. *Carbon* **1964**, *1*, 209–214.
- (3) Evans, E. L.; Griffiths, R. J. M.; Thomas, J. M. *Science* **1971**, *171*, 174–175.
- (4) Hennig, G. R. *J. Chem. Phys.* **1964**, *40*, 2877–2882.
- (5) Chang, H.; Bard, A. J. *J. Am. Chem. Soc.* **1990**, *112*, 4598–4599.
- (6) Chu, X.; Schmidt, L. D. *Carbon* **1991**, *29*, 1251–1255.
- (7) Tracz, A.; Wegner, G.; Rabe, J. P. *Langmuir* **1993**, *9*, 3033–3038.
- (8) Clemmer, C. R.; Beebe, T. P., Jr. *Science* **1991**, *251*, 640–642.
- (9) Patrick, D. L.; Cee, V. J.; Beebe, T. P., Jr. *Science* **1994**, *265*, 231–234.
- (10) Patrick, D. L.; Cee, V. J.; Purcell, T. J.; Beebe, T. P., Jr. *Langmuir* **1996**, *12*, 1830–1835.
- (11) Zeglinski, D. M.; Ogletree, D. F.; Beebe, T. P., Jr.; Hwang, R. Q.; Somorjai, G. A.; Salmeron, M. B. *Rev. Sci. Instrum.* **1990**, *61*, 3769–3774.
- (12) Dr. A. W. Moore, personal communication.
- (13) Chang, H.; Bard, A. J. *J. Am. Chem. Soc.* **1991**, *113*, 5588–5596.
- (14) Yang, R. T.; Wong, C. *J. Chem. Phys.* **1981**, *75*, 4471–4476.
- (15) McCarroll, B.; McKee, D. W. *Nature* **1970**, *225*, 722–723.
- (16) Chu, X.; Schmidt, L. D. *Surf. Sci.* **1992**, *268*, 325–332.
- (17) Tandon, D.; Hippo, E. J.; Marsh, H.; Sebok, E. *Carbon* **1997**, *35*, 35–44.
- (18) Bräuchle, G.; Richard-Schneider, S.; Illig, D.; Rockenberger, J. *Appl. Phys. Lett.* **1995**, *67*, 52–54.
- (19) Bräuchle, G.; Richard-Schneider, S.; Illig, D.; Beck, R. D.; Schreiber, H.; Kappes, M. M. *Nucl. Instrum. Methods Phys. Res. B* **1996**, *112*, 105–108.
- (20) Reimann, C. T.; Sullivan, P. A.; Türpitz, A.; Altmann, S.; Quist, A. P.; Bergman, A.; Oscarsson, S. O.; Sundqvist, B. U. R.; Håkansson, P. *Surf. Sci.* **1995**, *341*, L1019–L1024.
- (21) Wong, C.; Yang, R. T. *Carbon* **1982**, *20*, 253–4.
- (22) Thomas, J. M.; Roscoe, C. In *Chemistry and Physics of Carbon*; Walker, P. L., Jr. Ed.; Marcel Dekker: New York, 1968; Vol. 3, pp 1–44.
- (23) Hennig, G. R. *Science* **1965**, *147*, 733–734.
- (24) The Z piezo was calibrated by measuring the height of many monolayer HOPG steps. A histogram of these measurements showed a peak centered at 3.44 Å, but with considerable breadth ($\sigma = \pm 1$ Å), possibly due to varying amounts of sample compressibility.
- (25) At 725 °C and below no new monolayer pits formed during oxidation, while at 800 °C some new pits did form during oxidation. This was insignificant for shorter etch times (1 and 2 min), but for the longest etch time (3 min) only the largest one-third of the observed monolayer etch pits were used in calculations.
- (26) Yang, R. T.; Wong, C. *Science* **1981**, *214*, 437–438.
- (27) Yang¹⁴ used a formula of reactions per edge carbon per second = $0.938 \cdot dr/dt$ (dr/dt = rate of change in pit radius in Å·s⁻¹). Using slightly different methods, we derived a similar formula of $0.763 \cdot dr/dt$ (this value is partly dependent on the value chosen for edge atoms per unit perimeter, which depends on the details of the edge geometry).
- (28) McKee, D. W.; Spiro, C. L. *Carbon* **1985**, *23*, 437–444.
- (29) Radovic, L. R.; Walker Jr., P. L. *Fuel Process. Technol.* **1984**, *8*, 149–154.
- (30) Gerasimov, V. V.; Gerasimova, V. V.; Samoilov, A. G. *Dokl. Akad. Nauk* **1991**, *321*, 150–152.
- (31) Prudnikov, A. P.; Brychkov, Y. A.; Marichev, O. I. *Integrals and Series*; Gordon and Breach: New York, 1986; Vol. 1, p 140.
- (32) Often in calculations such as this, only the kinetic energy normal to the surface is considered, since "glancing" collisions deliver little energy to a flat surface.⁴² In the present case, reaction occurs at step edges, rather than at a flat surface, so collisions need not be normal to the surface to be effective. Since explicit treatment of this issue is geometry dependent, we chose to use the total number of collisions. Including this geometry term would only lower the predicted reaction rate, further widening the gap between experimental and predicted values.
- (33) Ahmed, S.; Back, M. H. *Carbon* **1985**, *23*, 513–524.
- (34) Spokes, G. N.; Benson, S. W. In *Fundamentals of Gas-Surface Interactions*; Saltsburg, H., Smith, J. N., Jr., Rogers, M., Eds.; Academic Press: New York, 1967; pp 318–329.
- (35) Horton, W. S. Oxidation kinetics of pyrolytic graphite. *Proceedings of the Fifth Carbon Conference*; Pergamon: New York, 1962; pp 233–241.
- (36) Stevens, F.; Beebe, T. P., Jr. *Comput. Chem.*, in press.
- (37) Yang, R. T. In *Chemistry and Physics of Carbon*; Thrower, P. A., Ed.; Marcel Dekker: New York, 1984; Vol. 19, pp 163–210.
- (38) Rodríguez-Reinoso, F.; Thrower, P. A.; Waker, P. L., Jr. *Carbon* **1974**, *12*, 63–70.
- (39) Gulbrandsen, E. A.; Andrew, K. F. *Ind. Eng. Chem.* **1952**, *44*, 1034–1038.
- (40) Walker, P. L., Jr.; Vastola, F. J.; Hart, P. J. In *Fundamentals of gas-surface interactions*; Saltsburg, H., Smith, J. N., Jr., Rogers, M., Eds.; Academic Press: New York, 1967; pp 307–317.
- (41) Stevens, F.; Buehner, D.; Beebe, T. P., Jr. *J. Phys. Chem. B* **1997**, *101*, 6491–6496.
- (42) Rettner, C. T.; Pfnür, H. E.; Auerbach, D. J. *Phys. Rev. Lett.* **1985**, *54*, 2716–2719.